Article

Cell Reports

Aß Facilitates LTD at Schaffer Collateral Synapses Preferentially in the Left Hippocampus

Graphical Abstract

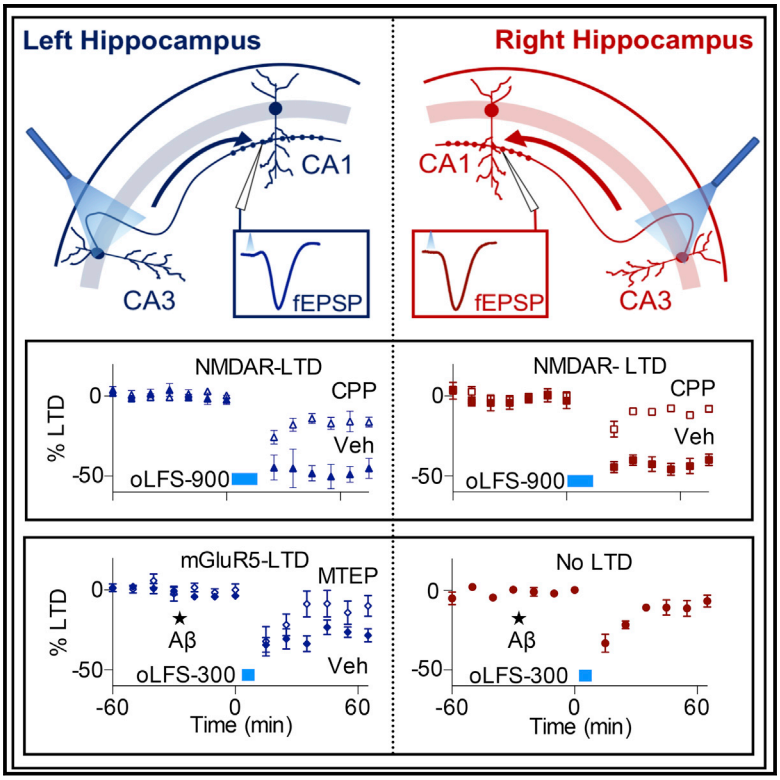

Authors

Kenneth J. O'Riordan, Neng-Wei Hu, Michael J. Rowan

Correspondence

hunw@tcd.ie (N.-W.H.), mrowan@tcd.ie (M.J.R.)

In Brief

O'Riordan et al. find that a form of long-term synaptic plasticity, LTD, can be induced by diffuse activation of specific excitatory inputs to the CA1 area of the living rat. Alzheimer's disease amyloid-β promotes this LTD, preferentially in the left hippocampus.

Highlights

- Diffuse optical low-frequency stimulation induces LTD at CA3-CA1 synapses *in vivo*
- oLTD requires the GluN2B subunit and ion channel function of the NMDA receptor
- oLTD is not facilitated by boosting acetylcholine or mGlu5 receptor activation
- At left CA3-CA1 synapses, Aß facilitates oLTD that now needs mGluR5

O'Riordan et al., 2018, Cell Reports *22*, 2053–2065
February 20, 2018
https://doi.org/10.1016/j.celrep.2018.01.085

CellPress

Cell Reports
Article

Aß Facilitates LTD at Schaffer Collateral Synapses Preferentially in the Left Hippocampus

Kenneth J. O'Riordan,[1,3] Neng-Wei Hu,[1,2,3,*] and Michael J. Rowan[1,4,*]
[1]Department of Pharmacology and Therapeutics and Institute of Neuroscience, Watts Building, Trinity College, Dublin 2, Ireland
[2]Department of Gerontology, Yijishan Hospital, Wannan Medical College, Wuhu, China
[3]These authors contributed equally
[4]Lead Contact
*Correspondence: hunw@tcd.ie (N.-W.H.), mrowan@tcd.ie (M.J.R.)
https://doi.org/10.1016/j.celrep.2018.01.085

SUMMARY

Promotion of long-term depression (LTD) mechanisms by synaptotoxic soluble oligomers of amyloid-β (Aß) has been proposed to underlie synaptic dysfunction in Alzheimer's disease (AD). Previously, LTD was induced by relatively non-specific electrical stimulation. Exploiting optogenetics, we studied LTD using a more physiologically diffuse spatial pattern of selective pathway activation in the rat hippocampus *in vivo*. This relatively sparse synaptic LTD requires both the ion channel function and GluN2B subunit of the NMDA receptor but, in contrast to electrically induced LTD, is not facilitated by boosting endogenous muscarinic acetylcholine or metabotropic glutamate 5 receptor activation. Although in the absence of Aß, there is no evidence of hippocampal LTD asymmetry, in the presence of Aß, the induction of LTD is preferentially enhanced in the left hippocampus in an mGluR5-dependent manner. This circuit-selective disruption of synaptic plasticity by Aß provides a route to understanding the development of aberrant brain lateralization in AD.

INTRODUCTION

The disruption of mechanisms underlying the plasticity of excitatory synaptic transmission, including long-term potentiation (LTP) and long-term depression (LTD), is believed to mediate impairment of critical brain functions such as certain forms of hippocampus-dependent learning and memory in many psychiatric and neurological disorders (Collingridge et al., 2010; Titley et al., 2017). In particular, key neuropathological proteins of Alzheimer's disease (AD), amyloid-β (Aß), and tau form soluble oligomers that potently and selectively interfere with cellular processes underlying plasticity throughout the brain's vulnerable networks, including the hippocampus (Spires-Jones and Hyman, 2014). Indeed, the excessive promotion of hippocampal LTD mechanisms by synaptotoxic soluble Aß has been proposed to provide a likely functional basis for deficits in cognition in AD, potentially independent of amyloid plaque and neurofibrillary tangle pathology (Collingridge et al., 2010; Koss et al., 2016; Sperling et al., 2014).

In contrast to LTP, the study of LTD in the adult rodent hippocampus has proven challenging, particularly in *vivo* (Errington et al., 1995; Staubli and Scafidi, 1997), making its physiological relevance open to debate (Andersen et al., 2017). Concordantly, the standard electrical low-frequency stimulation (eLFS, consisting of a set of 900 pulses at 1 Hz) protocol, used to study NMDA receptor (NMDAR)-dependent LTD at CA3-to-CA1 synapses in immature hippocampal slices, can induce LTD in anesthetized or freely behaving adult rats in a manner that is strongly dependent on experimental conditions (Fox et al., 2006; Kemp and Manahan-Vaughan, 2004; Wong et al., 2007; Xu et al., 1997). Recently, we reported that high-intensity eLFS reliably induced robust input-selective, muscarinic acetylcholine receptor (AChR)-dependent LTD in the hippocampus of anesthetized rats (Hu et al., 2014). Because electrical field stimulation activates pathways *en masse* and relatively indiscriminately, the requirement for high-intensity pulses was attributed to a need to activate cholinergic, in addition to glutamatergic, fibers during the eLFS (Caruana et al., 2011). Moreover, standard electrical pulses stimulate synapses densely, increasing the likelihood that glutamate spillover from nearby synapses will activate peri/extra-synaptic glutamate receptors (Arnth-Jensen et al., 2002; Scimemi et al., 2004). In accordance, activation of metabotropic glutamate 5 receptors (mGluR5s), known to be primarily located at peri-synaptic sites (Luján et al., 1997), had a strong positive modulatory effect on LTD induction by eLFS (K.J. O'Riordan et al., 2017, BNA, abstract PW115). Unlike electrically evoked activity, natural spatial patterns of activation are relatively sparse during normal hippocampal mnemonic function (Ramirez et al., 2013), raising the question of whether cross-talk via peri/extra-synaptic glutamate receptors occurs under physiological conditions.

At the circuit level, the structure and function of the hippocampus are lateralized in health and disease (Concha et al., 2012). Shifts in hippocampal asymmetry are exacerbated with the insidious advance of AD (Douaud et al., 2013; Wachinger et al., 2016), but little is known regarding possible mechanisms. Elucidation of such circuit-level processes is a key challenge in AD research (De Strooper and Karran, 2016). Left and right CA3 pyramidal neurons form synapses with CA1 pyramidal neurons that have different morphology and glutamate receptor expression (Kawakami et al., 2003), underlying hippocampal asymmetry of memory and LTP (Kohl et al., 2011; Shipton et al., 2014) in the mouse hippocampus. Conditioning stimulation of left hippocampal CA3 pyramidal neurons preferentially

triggers LTP at apical dendrites on CA1 pyramidal neurons (Kohl et al., 2011; Shipton et al., 2014). Although it is unknown whether hippocampal LTD is asymmetric, Kawahara and colleagues (Kawahara et al., 2013) reported that LTD is more easily induced in slices from adult mice that congenitally express the type of apical synapse that right CA3 neurons form with CA1 in both hemispheres. This finding raises the prospect that, in healthy rodents, LTD may be preferentially induced at CA1 synapses formed by right CA3 pyramidal neurons. Aß oligomers facilitate eLFS-induced LTD by abnormal engagement of mGluR5 (Hu et al., 2014; Li et al., 2009), putatively by promoting the aberrant synaptic localization of mGluR5 (Renner et al., 2010). Given that mGluR5 levels have been reported to be higher on apical spines of mouse CA1 neurons receiving input from left CA3 pyramidal cells (Shinohara and Hirase, 2009), Aß-facilitated LTD may be preferentially induced at these synapses.

To address these questions, we used selective expression of channelrhodopsin in excitatory neurons to enable more diffuse synaptic activation of glutamatergic pathways while, at the same time, avoiding the direct activation of non-glutamatergic, including cholinergic, fibers. We found that diffuse activation of Schaffer collaterals (SCs) with the optical LFS (oLFS) of CA3 neurons expressing channelrhodopsin-2 triggered robust, input-selective LTD in the CA1 area. Such oLFS triggered a relatively pure NMDAR-dependent LTD that was independent of mGluR5s and muscarinic AChRs. Moreover, the GluN2B subunit and a functional ion channel in NMDARs were obligatory for LTD induction by optical stimulation *in vivo*. Although the induction of LTD did not appear lateralized, Aß-facilitated, mGluR5-dependent LTD was preferentially induced at left CA3 SC input to CA1, providing a key insight into the circuit-level pathophysiology of AD.

RESULTS

High-Intensity Optical LFS Induces LTD at CA3-to-CA1 Synapses *In Vivo*

In order to study the induction of LTD by relatively selective stimulation of glutamatergic input from CA3 to CA1 *in vivo*, we used optogenetics in the acutely anesthetized adult rat. To achieve this, we injected an adeno-associated virus (AAV) expressing channelrhodopsin-2 (hChR2(H134R)-EYFP [enhanced yellow fluorescent protein]) driven by the CaMKII promoter, which selectively promotes transduction in excitatory neurons, into the CA3 area. As can be seen in Figure 1A, at the time of recording, channelrhodopsin-2/EYFP fusion protein was present in CA3 pyramidal neurons, especially near the site of injection, but also the SC output in ipsilateral CA1 and the commissural outputs in the contralateral CA3 and CA1 areas. Although some CA2 pyramidal neurons were also transduced, less than 4% of input to CA1 *stratum radiatum* arises from these neurons (Shinohara et al., 2012). The expression of EYFP was relatively diffuse, with less than one in three cell bodies being clearly positive for EYFP (51 ± 7 cell bodies per millimeter, compared with 185 ± 9.5 DAPI-identified cell bodies per millimeter; $n = 6$; $p < 0.0001$, compared between groups; paired t test) (Figures 1B–1D).

With the optical fiber positioned over area CA3 ipsilateral to the side of virus injection (Figure 1E), optically evoked transmission at CA3-to-CA1 apical synapses was recorded in the ipsilateral *stratum radiatum* in the CA1 area (Figures 1F, 1G, 2A, 2B, S1A, and S1B). Responses in the optical pathway were stable for more than 4 hr, as indicated by the continuous monitoring of the response to test pulse stimulation and comparing the input-output relationship of stimulation intensity to field excitatory postsynaptic potential (fEPSP) amplitude at the start and end of the recording period. When compared with electrically evoked responses evoked by stimulation of SC/commissural fibers using an adjacent wire electrode (Figures S1C, S1D, S2A, and S2B), the sweep-to-sweep amplitude of the optically evoked responses appeared somewhat more variable, most likely because of variation in the number of channelrhodopsin 2 (ChR2) channels activated by each optical pulse.

The ability to induce LTD of optically evoked synaptic responses was assessed using a variety of low-frequency (1-Hz) protocols. Application of 900 optical pulses at an intensity that evoked 50% maximum fEPSPs only induced a transient depression of synaptic transmission that quickly reverted to pre-conditioning levels (Figures S3A and S3C). In contrast, a tetanus consisting of 900 pulses delivered at 75% maximum intensity triggered significant but small LTD (Figures S3B and S3D). In order to induce robust LTD, it was necessary to apply a stronger 900-pulse, 1-Hz protocol. Such LFS, at an intensity that evoked fEPSPs that were approximately 95% of the maximum (900 pulse optical LFS [oLFS-900]), triggered a large LTD of optically evoked test fEPSPs that remained stable for at least 3 hr (Figures 1F and 1H) and an associated shift of the input-output curve to the right (Figure 1H), similar to that induced by 900 pulse electrical LFS (eLFS-900) of a nearby mixed SC/commissural pathway (Figures S2A and S2C). Because the induction of LTP at CA3-to-CA1 synapses *in vitro* has been reported to be lateralized (Kohl et al., 2011; Shipton et al., 2014), we expected that the induction of LTD *in vivo* might be asymmetrical. However, the magnitude of LTD in the left and right SC inputs was not significantly different (left: 64.7 ± 2.1%; right: 67.2 ± 1.9%; values at 1 hr after oLFS-900, $n = 7$ for each side; $p < 0.0001$, compared with respective baselines; and $p > 0.99$, compared between the two sides, two-way ANOVA with repeated-measures with Bonferroni multiple comparison test; 2WA-RM-B) (Figures 2C and 2D).

If asymmetry of LTD at these synapses is dependent on the magnitude of LTD induced by oLFS, it may be more apparent using weaker oLFS protocols. However, a low-frequency conditioning stimulation containing 300 high-intensity pulses (oLFS-300, 1 Hz) caused similar magnitude short-term depression in the left or right hippocampus, failing to induce significant LTD on either side (left: 100.4 ± 1.0%, $n = 4$; right: 97.3 ± 1.4% at 1 hr, $n = 4$; $p = 0.69$ for right, and $p > 0.99$ for left, compared with respective baselines; and $p > 0.99$ between the two sides [2WA-RM-B]) (Figures 2E and 2F). When the number of high-intensity pulses was increased to 600 during conditioning stimulation, small and comparable magnitude LTD was induced in both the left and right sides. Thus, at 1 hr post-oLFS-600, the value of excitatory postsynaptic potential (EPSP) measured 82.8 ± 2.1% ($n = 4$) in the left hippocampus and 82.4 ± 4.7% ($n = 4$) in the right hippocampus ($p < 0.01$ on each side, compared with respective baselines; and $p > 0.99$, compared between sides; 2WA-RM-B) (Figures 2G and 2H).

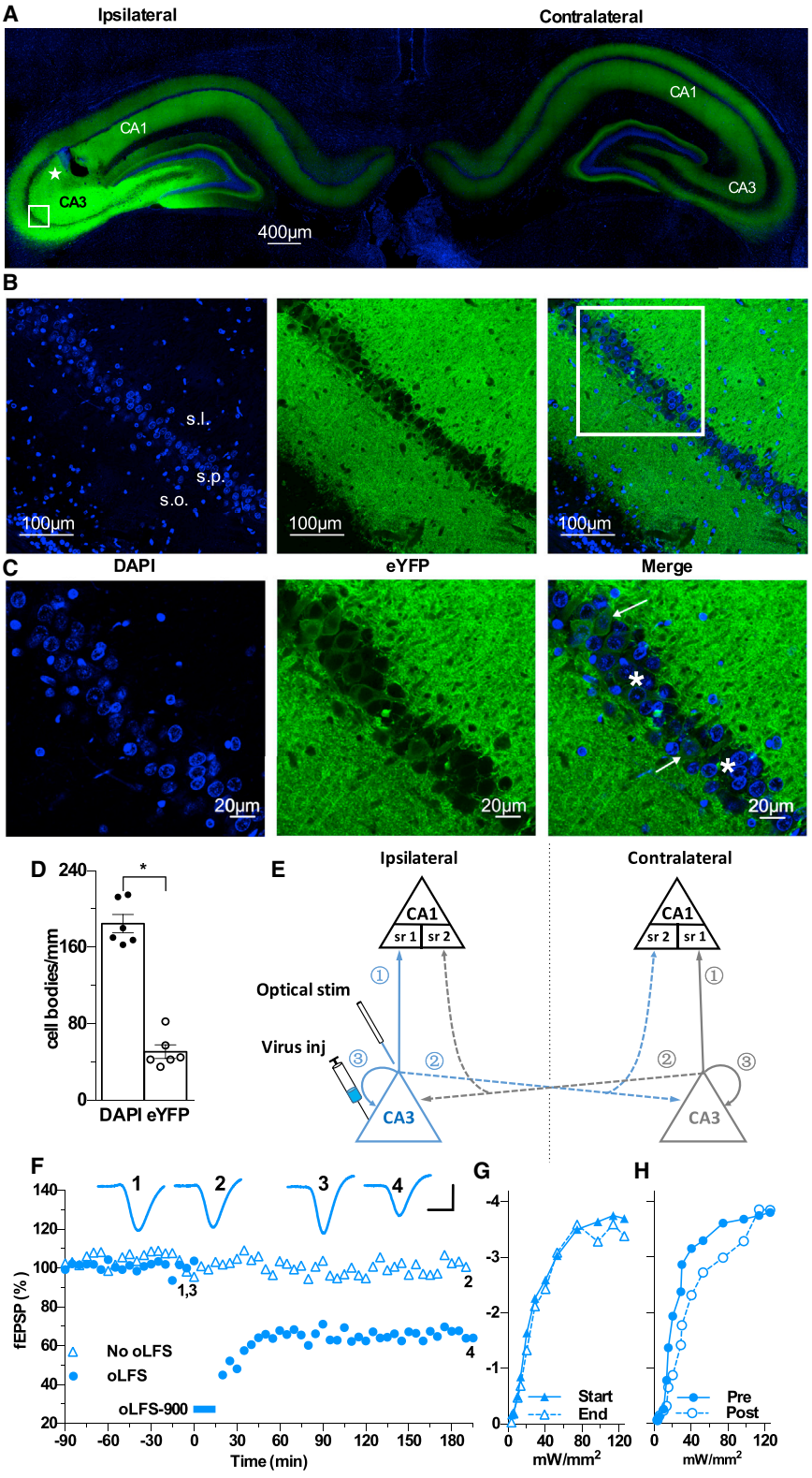

Figure 1. Channelrhodopsin Expression to Allow Relatively Diffuse Stimulation of CA3 Pyramidal Neuron Schaffer Collaterals that Induces Long-Term Depression *In Vivo*

(A) Representative confocal image showing EYFP fluorescence (green) indicating expression pattern of channelrhodopsin and DAPI stain (blue, cell bodies) in transverse brain sections; a star indicates the approximate location of the stimulation optrode ipsilateral to the side of virus injection. The box indicates the area shown in (B).

(B) Images of the CA3 area used to evaluate ChR2-EYFP expression near the site of virus injection. s.l., *stratum lucidum*; s.p., pyramidal cell body layer; s.o., *stratum oriens*. Scale bars, 100 μm. The box indicates the area shown in (C).

(C) High-resolution images showing examples of cells with (arrows) and without (asterisks) clear expression of ChR2-EYFP. Scale bars, 20 μm.

(D) The DAPI CA3 cell-body count near the optrode tip was significantly greater than the number of cell bodies clearly positive for EYFP (n = 6, 3 left/3 right). Values are expressed as mean percent ± SEM. *p < 0.05, paired t test.

(E) Schema showing how optical stimulation (stim) ipsilateral to the virus injection (inj) activates nearby CA3 neurons expressing ChR2 (blue) but not CA3 neurons originating in the non-injected hippocampus (contralateral, gray). Optically evoked responses recorded in the *stratum radiatum* (sr) of the ipsilateral CA1 area are generated by selective activation of SCs. In contrast, ipsilateral electrical stimulation non-specifically activates mixed SC and commissural evoked responses. (1) Schaffer collaterals. (2) Commissural fibers (dashed lines). (3) Recurrent collaterals.

(F) Representative examples of single experiments recording on right-side SC optically evoked responses to test pulse stimulation in an anesthetized adult rat, with or without additional optical low-frequency conditioning stimulation at high intensity (95% maximum) (oLFS-900; blue bars, 900 high-intensity pulses at 1 Hz). LTD of the optically evoked responses was induced in the animal that received oLFS.

(G) Input-output curves at the start and end of the recording period in the absence of oLFS.

(H) Input-output curves before (Pre) and ~3 hr after (Post) oLFS.

Insets show representative traces at the times indicated. Scale bars: vertical, 1 mV; horizontal, 10 ms.

See also Figures S1–S3.

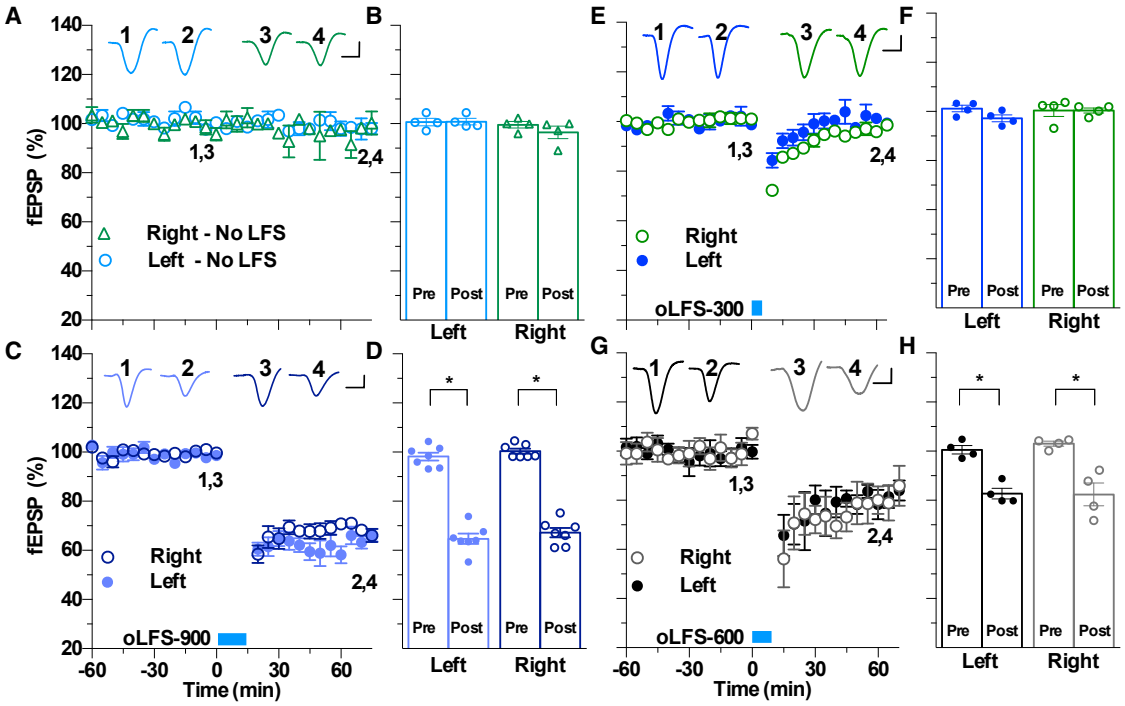

Figure 2. Symmetrical Induction of LTD at Left and Right CA3-to-CA1 Schaffer Collateral Synapses *In Vivo*

(A) Optically evoked responses are stable in the absence of oLFS in both right and left Schaffer collateral (SC) synapses.

(B) Summary of the mean fEPSP amplitude data in (A), at times equivalent to just before (Pre) and 1 hr after (Post) application of oLFS (left: 101.8 ± 2.7%; right: 96.1 ± 0.4% at 1 hr; n = 4 per side; $p > 0.99$, compared with respective Pre values; and $p = 0.22$, compared between sides; 2WA-RM-B).

(C) oLFS-900 (blue bar, 900 high-intensity pulses at 1 Hz) induced similar large-magnitude LTD in both hemispheres.

(D) Summary of the data in (C) just before (Pre) and 1 hr after (Post) oLFS.

(E) oLFS-300 (blue bar, 300 high-intensity pulses at 1 Hz) failed to induce LTD in either hemisphere.

(F) Summary of the data in (E) just before (Pre) and 1 hr after (Post) oLFS.

(G and H) oLFS-600 (blue bar, 600 high-intensity pulses at 1 Hz) induced similar small-magnitude LTD in both hemispheres (G). Data pre- and 1 hr post-oLFS are summarized in the bar chart (H).

Scale bars: vertical, 1 mV; horizontal, 10 ms. 2WA-RM-B. *$p < 0.05$.

See also Figures S1 and S3.

Input Selectivity of Optical LFS-Induced LTD *In Vivo*

In order to determine whether optical LFS-induced LTD (oLTD) *in vivo* is input selective, we tested whether the induction of LTD by oLFS of SC input to CA1 affected synaptic responses evoked by electrical stimulation of an apparently independent mixed SC/commissural input nearby (see Experimental Procedures), and vice versa. We applied high-intensity LFS to both pathways separately and continuously monitored, with a single recording electrode in the *stratum radiatum* in the CA1 area, fEPSPs evoked by alternate optical and electrical test pulses. As predicted, the expression of LTD in one pathway did not appear to affect responses in the other pathway after applying either oLFS or eLFS (Figure 3). Thus, the induction of LTD by a single train of high-intensity oLFS (optical: 71.6 ± 2.2% at 1 hr, n = 10, 4 left/6 right; $p < 0.0001$, compared with pre-LFS baseline, one-way ANOVA repeated-measures with Bonferroni multiple comparisons [1WA-RM-B]) did not affect baseline synaptic responses in the electrical pathway (electrical: 98.8 ± 1.4% at 1 hr, n = 10; $p > 0.99$, compared with pre-oLFS baseline) (Figures 3A and 3C). Similarly, in a separate group of animals, the induction of LTD by strong eLFS (electrical: 70.6 ± 3.3% at 1 hr, n = 9, 4 left/5 right; $p < 0.0001$, compared with pre-eLFS baseline) did not alter baseline optically evoked fEPSPs (optical: 99.5 ± 1.9% at 1 hr; $p = 0.59$, compared with pre-eLFS baseline) (Figures 3B and 3D).

Because a single LFS tetanus might not saturate LTD expression, we wondered whether repeated LFS of one pathway might influence the synaptic responses in the other pathway. Repeated application at 1-hr intervals of eLFS (Figures 3E and 3F; 2 left/2 right) or oLFS (Figures 3G and 3H; 3 left/1 right) did not significantly increase the magnitude of LTD in the same pathway. These data indicate that a single LFS-900 is sufficient to saturate LTD and confirm that the expressions of LTD in the optical and electrical pathways are effectively independent of each other.

We also examined whether the induction of LTD in one pathway was influenced by the prior induction of LTD in the other pathway following single or repeated LFS. The single (Figures 3A and 3C) or repeated (Figures 3G and 3H) application of oLFS did not significantly affect the subsequent ability to induce LTD with eLFS (65.5 ± 10.8%, n = 4; $p < 0.01$, compared with post-oLFS3 level; 1WA-RM-B). However, even though single eLFS did not significantly affect the subsequent induction of LTD in the optical

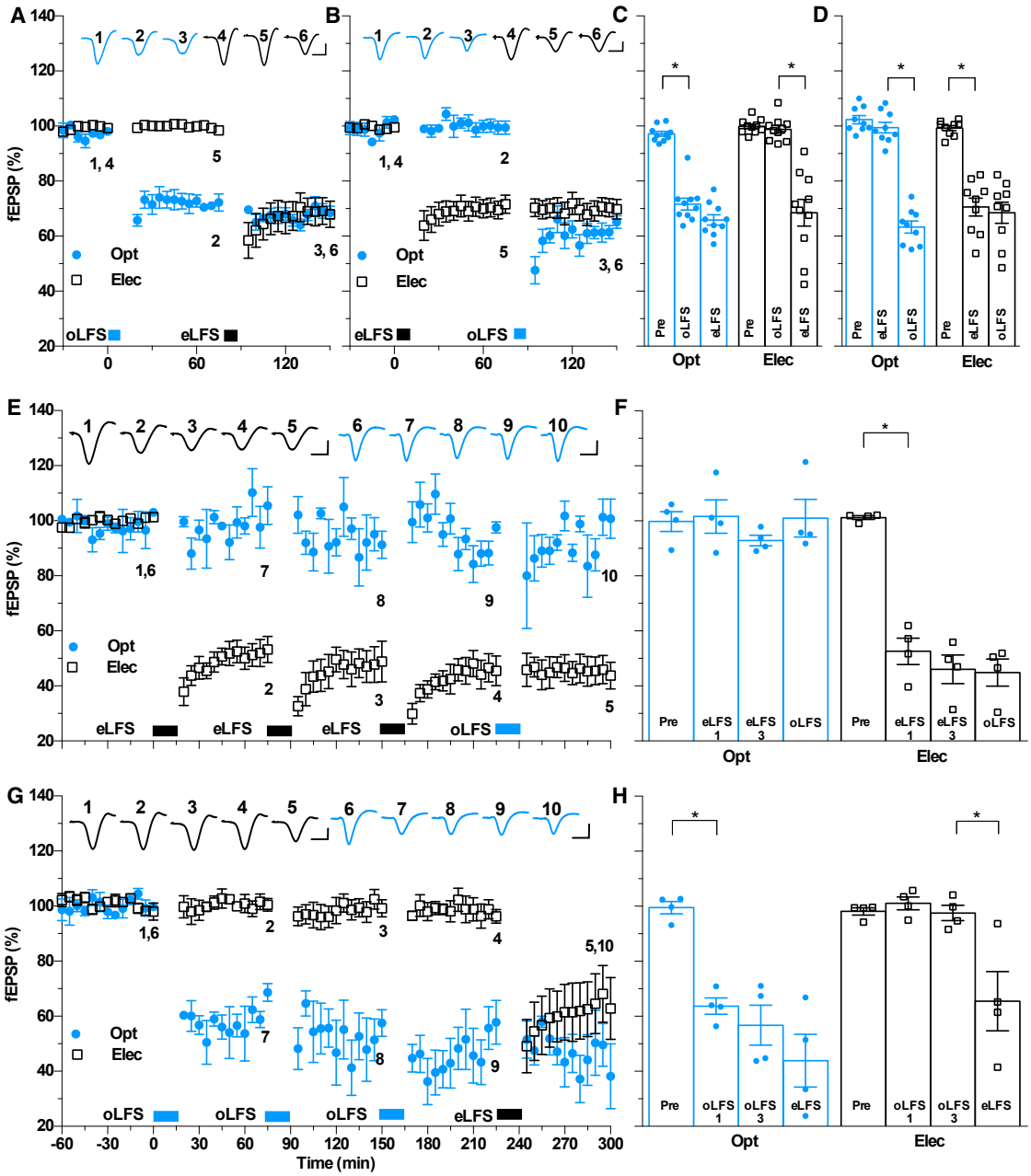

Figure 3. Input Selectivity of oLFS-Induced LTD *In Vivo*

(A) After 30 min of stable baseline recording from both optical (Opt, blue) and electrical (Elec, black) pathways in the same animal, application of oLFS (blue bars; 900 high-intensity pulses at 1 Hz, n = 10, 4 left/6 right) induced LTD of optical responses but did not affect responses in the electrical pathway. Subsequent application of eLFS (black bars; 900 high-intensity pulses at 1 Hz) only induced LTD of electrical responses but did not affect responses in the optical pathway.

(B) Similarly, when the conditioning stimulation sequence was reversed, LTD in one pathway did not affect responses in the other pathway (n = 9, 4 left/5 right).

(C and D) Bar charts summarizing the data in both pathways for before (Pre) and 1 hr after each set of conditioning stimulation in (A) (shown in C) and in (B) (shown in D).

(E–H) Similarly, the application of repeated LFS to one pathway, to ensure LTD saturation, also failed to affect the responses recorded in the other pathway. However, although repeated oLFS (blue bars, 900 high-intensity pulses at 1 Hz, n = 4, 3 left/1 right, in G and H) did not affect subsequent LTD induction by eLFS (black bars, 900 high-intensity pulses at 1 Hz), the induction of LTD in the optical pathway by oLFS 1 hr after the third eLFS was inhibited (n = 4, 2 left/2 right, in E and F).

Scale bars: vertical, 1 mV; horizontal, 10 ms. 1WA-RM-B. *p < 0.05.

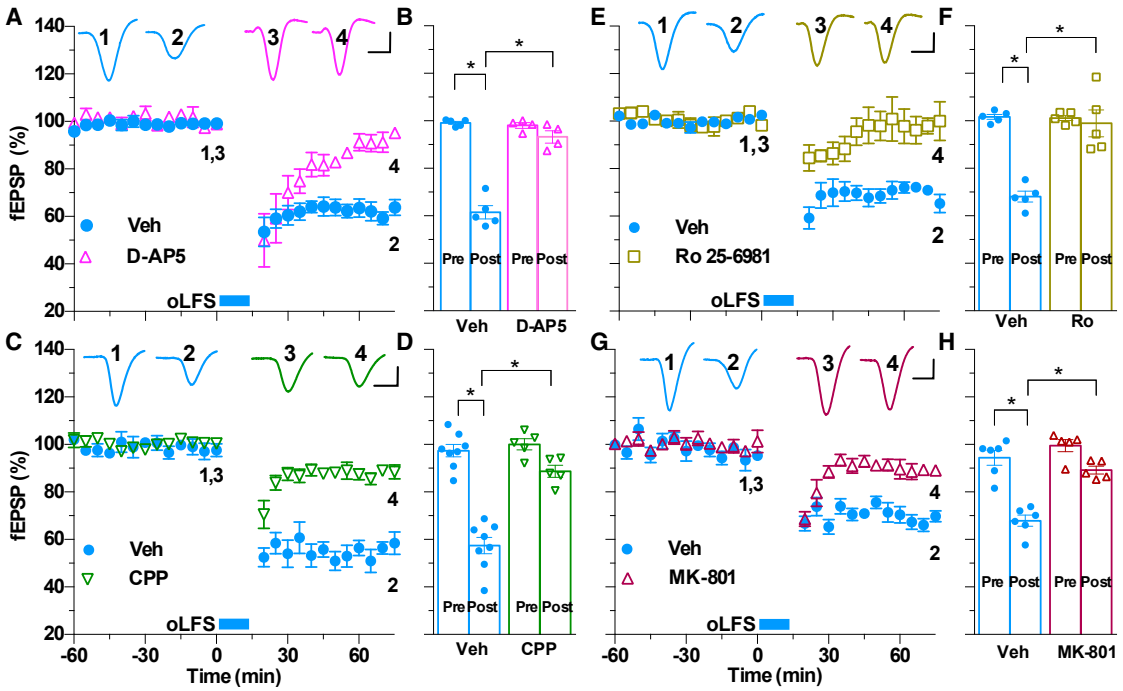

Figure 4. NMDAR Dependence of the Induction of oLTD *In Vivo*

(A and B) The competitive NMDAR antagonist D-AP5 (100 nmol, i.c.v., 10 min pre-oLFS) inhibited oLTD by oLFS (blue bar, 900 high-intensity optical pulses at 1 Hz) (A). Values just before (Pre) and 1 hr post-oLFS (Post) are presented in the bar chart (B) (control: n = 5, 1 left/4 right; D-AP5: n = 4, 3 left/1 right).

(C and D) The competitive NMDAR antagonist CPP (10 mg/kg, i.p., 2.25 hr pre-oLFS) attenuated oLTD (C). Values at 1 hr post-LFS are presented in the bar chart (D) (control: n = 8, 4 left/4 right; CPP: n = 5, 3 left/2 right).

(E and F) Similarly, systemic administration of the non-competitive GluN2B subtype-selective NMDAR antagonist Ro 25-6981 (6 mg/kg, i.p.) abrogated oLTD (E). Values at 1 hr post-LFS (control: n = 5, 2 left/3 right; Ro 25-6981: n = 5, 2 left/3 right) are presented in the bar chart (F).

(G and H) Moreover, the use-dependent NMDAR ion channel blocker MK-801 potently (0.5 mg/kg, i.p.) inhibited oLTD. Values at 1 hr post-LFS (control: n = 6, 3 left/3 right; MK-801: n = 5, 2 left/3 right) are presented in the bar chart (H).

Scale bars: vertical, 1 mV; horizontal, 10 ms. 2WA-RM-B. *p < 0.05.

pathway (Figures 3B and 3D), three sets of eLFS greatly impeded the subsequent ability to induce oLTD (101.0 ± 6.8%, n = 4; p = 0.81, compared with post-eLFS3 level) (Figures 3E and 3F).

NMDAR Dependence of oLTD *In Vivo*

Previously we reported that the induction of LTD by eLFS (eLTD), consisting of 900 high-intensity pulses at 1 Hz, is only blocked by high local intracerebral doses of NMDAR antagonists when given alone, whereas standard systemic doses of NMDAR antagonists were only effective if mGluR5 was simultaneously blocked (Hu et al., 2014; K.J. O'Riordan et al., 2017, BNA, abstract PW115). In order to determine whether activation of NMDARs is needed for the induction of oLTD *in vivo*, we investigated standard doses of the competitive antagonists D-AP5 and CPP. As shown in Figures 4A and 4B, treatment with D-AP5 (100 nmol, intracerebroventricularly [i.c.v.], 10 min pre-LFS), significantly attenuated the induction of oLTD (control: 61.5 ± 2.8%, n = 5; 1 left/4 right; p < 0.0001, compared with baseline and between groups; D-AP5: 93.2 ± 2.6%, n = 4; 3 left/1 right; p = 0.79, compared with baseline; 2WA-RM-B). Similarly, CPP (10 mg/kg, intraperitoneally [i.p.], 2 hr pre-LFS) prevented the induction of oLTD (control: 57.4 ± 3.5%, n = 8, 4 left/4 right; p < 0.0001, compared with baseline and between groups; CPP: 88.7 ± 2.5%, n = 5, 3 left/2 right; p = 0.12, compared with baseline; 2WA-RM-B) (Figures 4C and 4D). Next, we studied the non-competitive GluN2B subunit-selective negative allosteric modulator Ro 25-6981, because GluN2B has been implicated in mediating eLTD induction *in vivo* (Fox et al., 2006; Wong et al., 2007). Ro 25-6981 (6 mg/kg, i.p., 1 hr pre-LFS) also blocked oLTD (control: 68.1 ± 2.3%, n = 5, 2 left/3 right; Ro 25-6981: 99.0 ± 5.7%, n = 5, 2 left/3 right; p > 0.99, compared with baseline; p < 0.001, compared between groups) (Figures 4E and 4F).

In the light of the controversy over the requirement for ion flux through the NMDAR channel in eLTD induction *in vitro* (Babiec et al., 2014; Nabavi et al., 2013), we also examined the effect of the use-dependent NMDAR channel blocker MK-801. A relatively low dose of MK-801 (0.5 mg/kg, i.p., 1 hr pre-LFS) inhibited the induction of oLTD (control: 67.9 ± 2.3%, n = 6, 3 left/3 right; MK-801: 89.2 ± 1.7%, n = 5, 2 left/3 right; p < 0.0001, compared between groups and with baseline for control; p = 0.086, compared with baseline for MK-801) (Figures 4G and 4H).

Summarizing these results, the induction of synaptic LTD by optical stimulation of glutamatergic fibers *in vivo* was blocked by relatively low doses of NMDAR antagonists that act at either the orthosteric glutamate binding site (D-AP5 and CPP), the

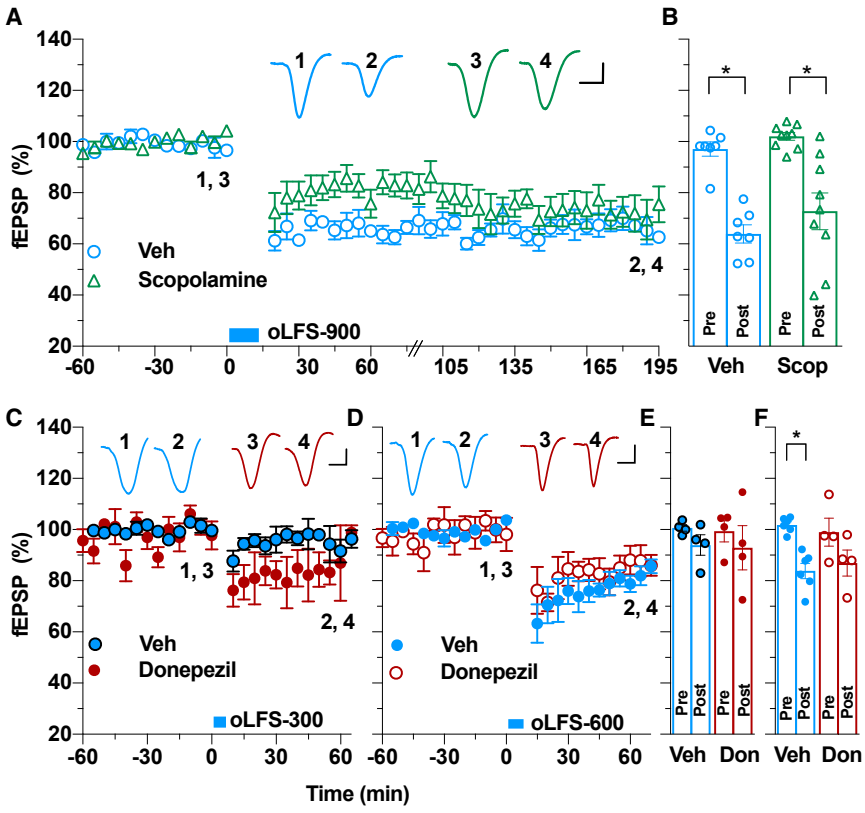

Figure 5. Lack of Cholinergic Influence on oLTD *In Vivo*

(A and B) The muscarinic acetylcholine receptor antagonist scopolamine (0.2 mg/kg, i.p., 1 hr pre-LFS, n = 9, 5 left/4 right) had little effect on LTD induced by oLFS-900 (blue bar, 900 high-intensity pulses at 1 Hz, n = 7, 4 left/3 right) (A). Values at 3 hr post-LFS are presented in the bar chart (B).

(C–F) Similarly, the anticholinesterase donepezil (1 mg/kg s.c., 1 hr pre-LFS) had little effect on LTD induction by oLFS-300 (blue bar, 300 high-intensity pulses at 1 Hz; control: n = 4, 1 left/3 right; donepezil: n = 4, 1 left/3 right) (C and E) or oLFS-600 (blue bar, 600 high-intensity pulses at 1 Hz; control: n = 6, 3 left/3 right; donepezil: n = 4, 3 left/1 right) (D and F). Values at 1 hr post-LFS are presented in the bar charts.

Scale bars: vertical, 1 mV; horizontal, 10 ms. 2WA-RM-B. *p < 0.05.

See also Figure S4.

negative allosteric site on the GluN2B subunit (Ro 25-6981), or the NMDAR ion channel (MK-801).

Role of Cholinergic Transmission in oLFS Induction of LTD *In Vivo*

Previously, we reported that cholinergic transmission, via muscarinic acetylcholine receptors, lowered the threshold for LTD induction by high-intensity electrical stimulation and was required for LTD persistence beyond 3 hr in the *stratum radiatum* of the CA1 area (Hu et al., 2014). We hypothesized that such strong eLFS activated infiltrating cholinergic fibers to promote LTD. In the present experiments, we used optical stimulation to relatively selectively activate CA3 neurons. Therefore, we predicted that oLTD should be relatively independent of cholinergic input. First, we assessed whether the muscarinic acetylcholine (ACh) receptor (AChR) antagonist scopolamine blocked oLTD, since we previously found it to block LTD 3 hr after its induction by electrical LFS-900 of SC/commissural inputs (Hu et al., 2014). Although LTD in the optical pathway appeared to be variable in scopolamine-treated (0.2 mg/kg, i.p., 1–2 hr pre-LFS) animals, overall, there was no significant reduction of LTD magnitude at 3 hr post-oLFS (scopolamine: 72.8 ± 7.2%, n = 9; control: 63.9 ± 3.5%, n = 7; 4 left/3 right; $p < 0.001$, compared with baseline; and $p > 0.99$, between groups; 2WA-RM-B) (Figures 5A and 5B). When we compared the magnitude of oLTD between sides, because cholinergic input to the hippocampus may be lateralized (Kristofiková et al., 2004), we did not find a significant difference (left: 69.2 ± 9.2%, n = 5; right: 77.2 ± 12.5%, n = 4; $p > 0.99$, between groups; 2WA-RM-B).

Previously, we reported that donepezil, an anticholinesterase that boosts endogenous acetylcholine, lowered the threshold for the induction of LTD by a peri-threshold eLFS conditioning protocol. Therefore, we examined the effect of donepezil on the ability of relatively weaker oLFS protocols to induce LTD. oLFS-300 failed to induce LTD in the absence or presence of donepezil (1 mg/kg, subcutaneously [s.c.]) (control: 94.0 ± 4.0% at 1 hr, n = 4, 1 left/3 right; donepezil: 92.9 ± 8.7% at 1 hr, n = 4, 1 left/3 right; $p > 0.99$, compared with baseline and between groups; 2WA-RM-B) (Figures 2E, 2F, 5C, and 5E). We also assessed the ability of donepezil to enhance LTD induced by oLFS-600, which induced sub-maximal LTD (Figures 2G, 2H, 5D, and 5F). However, the magnitude of this submaximal LTD was not significantly enhanced by donepezil treatment (control: 83.8 ± 3.0% at 1 hr, n = 6, 3 left/3 right; $p < 0.01$, compared with baseline; donepezil: 86.7 ± 5.0%, n = 4, 3 left/1 right; $p = 0.25$, compared with baseline; and $p > 0.99$, compared with control; 2WA-RM-B).

Importantly, in interleaved experiments, we confirmed our earlier report that the same dose of scopolamine significantly inhibited eLTD (Figures S4A and S4B). In interleaved experiments, we also confirmed our previous finding that, whereas eLFS-300 alone caused little change from baseline, the same protocol induced robust synaptic LTD in the presence of donepezil (Figures S4C and S4D).

Role of mGlu Receptors in the Induction of Hippocampal oLTD *In Vivo*

Previously, we found that the induction of eLTD was regulated by mGluR5 (K.J. O'Riordan et al., 2017, BNA, abstract PW115). Such regulation is likely due to glutamate spillover, since mGluR5s are mainly located extrasynaptically. We explored

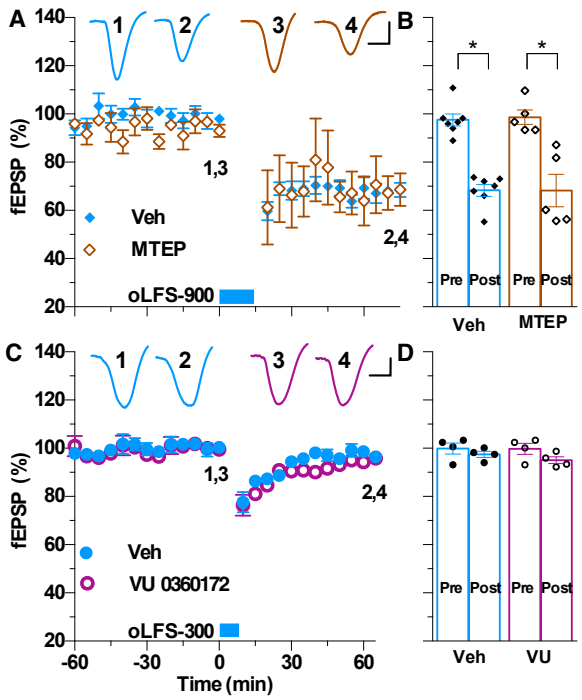

Figure 6. mGlu5 Receptor Independence of oLTD *In Vivo*

(A and B) The mGluR5 negative allosteric modulator MTEP (3 mg/kg, i.p.) (n = 5, 3 left/2 right) did not significantly affect the induction of oLTD by oLFS-900 (blue bar, 900 high-intensity pulses at 1 Hz) (n = 7, 3 left/4 right) (A). Values at 1 hr post-LFS are presented in the bar chart (B).

(C and D) The mGluR5 positive allosteric modulator VU 0360172 (15 mg/kg, s.c.) (n = 4, 2 left/2 right) did not facilitate the induction of LTD by a peri-threshold optical LFS conditioning protocol, oLFS-300 (blue bar, 300 high-intensity pulses at 1 Hz) (C). Values at 1 hr post-LFS (n = 4, 2 left/2 right) are presented in the bar chart (D).

Calibration bars: vertical, 1 mV; horizontal, 10 ms. 2WA-RM–B. *p < 0.05.

See also Figures S5 and S6.

the influence of mGluR5s on more diffuse synaptic LTD by testing the effects of negative and positive allosteric modulators of the receptor on oLFS induction of LTD. The mGluR5 negative allosteric modulator 3-((2-methyl-1,3-thiazol-4-yl)ethynyl)pyridine hydrochloride (MTEP) (3 mg/kg, i.p.) did not significantly affect the induction of oLTD (Figures 6A and 6B) (MTEP: 68.3 ± 6.7%, n = 5, 3 left/2 right; control: 68.3 ± 2.4%, n = 7, 3 left/4 right; $p < 0.001$ and < 0.0001, compared with respective pre-oLFS baselines; $p > 0.99$, between groups; 2WA-RM-B). The LTD induced in the presence of MTEP remained stable, as assessed in a subgroup of animals recorded over a 3-hr post-LFS period (Figures S5A and S5B). Moreover, pharmacologically boosting endogenous glutamate activation of mGluR5s with a positive allosteric modulator VU 0360172 (15 mg/kg, s.c., 1 hr pre-LFS) did not facilitate the induction of LTD by the oLFS-300. Thus, oLFS-300 induced a short-term depression of synaptic transmission either in the absence or presence of VU 0360172 (Figures 6C and 6D) (control: 97.5 ± 1.3% at 1 hr, n = 4, 2 left/2 right; $p > 0.99$, compared with baseline; VU 0360172: 95.1 ± 1.4%, n = 4, 2 left/2 right; $p = 0.62$, compared with baseline; and $p > 0.99$, between groups). We also assessed the ability of VU 0360172 to enhance LTD induced by oLFS-600 (Figures S5C and S5D). However, the magnitude of this submaximal LTD was not significantly enhanced by VU 0360172 treatment.

Similarly, since group II mGlu receptors (mGluRs) are located mainly extrasynaptically, we tested their role in oLTD induction. The mGlu2/3R antagonist LY341495, which also has high affinity for group III receptors (Bond et al., 2000; Kingston et al., 1998; Ornstein et al., 1998), failed to significantly affect the magnitude of oLTD at a dose (3 mg/kg, i.p.) that is unlikely to be totally selective for group II mGluRs (Figures S6A and S6B; see also Supplemental Experimental Procedures).

Lateralization of AD Aß-Facilitated LTD

We wondered whether the disruption of hippocampal synaptic plasticity by synaptotoxic oligomers of Aß may contribute to the reported lateralization of hippocampal dysfunction in AD. Specifically, we predicted that, since Aß-facilitated LTD is mGluR5 dependent (Hu et al., 2014), and rodent mGluR5 levels are higher on apical spines of CA1 neurons receiving input from left CA3 pyramidal cells (Shinohara and Hirase, 2009), Aß may preferentially facilitate LTD induction at these synapses. Synaptotoxic Aß oligomers diffuse rapidly into the hippocampus when injected i.c.v. (Kasza et al., 2017). We tested the ability of a dose of Aß that did not affect baseline transmission (Figures S7A and S7B) to facilitate the effects of the weak optical LFS (oLFS-300), which, on its own, failed to induce significant LTD (combined control group: 97.6 ± 1.8%, n = 11, 4 left/7 right, at 1 hr post-oLFS; $p > 0.99$, compared with baseline) (Figures 7A and 7B). Application of oLFS-300 30 min after injection of human Aß1-42 oligomers (1.2 nmol, i.c.v.) now triggered significant LTD (Aß: 82.6 ± 3.9%, n = 14; $p < 0.001$, compared with baseline and between groups; 2WA-RM-B) (Figures 7A and 7B). Importantly, there was clear evidence of lateralization of the disruptive effect of Aß. When we compared the magnitude of depression on the left and right sides of animals that had been recorded for 1 hr, we found that Aß preferentially facilitated the induction of LTD by oLFS at SCs in the left hippocampus (Aβ-left: 71.9 ± 3.8% at 1 hr post-oLFS%; $p < 0.01$, compared with baseline; Aβ-right: 93.4 ± 3.8%; $p = 0.56$, compared with baseline; n = 7 for both left and right; $p < 0.0001$, compared between groups, one-way ANOVA-Bonferroni and Bonferroni-corrected paired t) (Figures 7C and 7D). Importantly, in animals pre-injected with the mGluR5 negative allosteric modulator MTEP (3 mg/kg, i.p., 30 min before Aß), Aß no longer facilitated the induction of LTD by application of oLFS-300 to the left SC pathway (Aß + MTEP: 90.0 ± 6.6% at 1 hr, n = 6; $p = 0.32$, compared with pre-LFS, one-way ANOVA-Bonferroni and Bonferroni-corrected paired t) (Figures 7C and 7D). In order to determine whether the asymmetry in Aß-facilitated LTD was pathway selective, we compared the magnitude of LTD induced by a peri-threshold electrical LFS protocol (eLFS-300) after Aß injection ipsilateral to the stimulation and recording electrodes (Figures S7C and S7D). There was no evidence for lateralization of the effects of Aß on the induction of eLTD in the mixed SC/commissural pathway (Figures S7E and S7F).

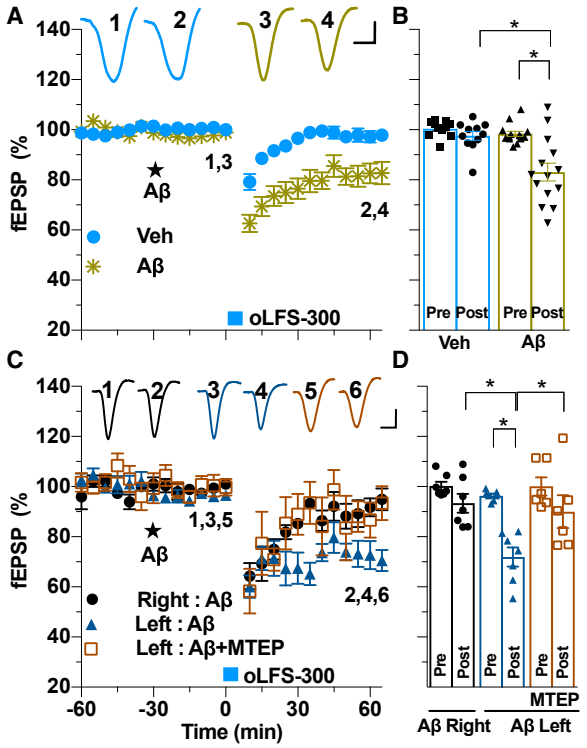

Figure 7. Lateralization of Alzheimer's Disease Aß-Facilitated LTD

(A and B) Injection of Aß (1.2 nmol, i.c.v.) 30 min before oLFS-300 (blue bar, 300 high-intensity pulses at 1 Hz) (n = 14, 7 left/7 right) enabled the induction of LTD (vehicle [Veh]: n = 11, 4 left/7 right) (A). Values at 1 hr post-LFS are presented in the bar chart (B).

(C and D) Remarkably, the facilitatory effect of Aß was lateralized so that oLFS-300 induced synaptic LTD at SCs in the left, but not right, hippocampus. Furthermore, Aß failed to induce LTD at left SC synapses in animals that had been pre-injected with the mGluR5 negative allosteric modulator MTEP (3 mg/kg, i.p.) (n = 6, all left) (C). Values at 1 hr post-LFS are presented in the bar chart (D).

Scale bars: vertical, 1 mV; horizontal, 10 ms. One-way ANOVA-Bonferroni and Bonferroni-corrected paired t. *p < 0.05.

See also Figure S7.

DISCUSSION

The relatively selective and diffuse expression of ChR2 in CA3 pyramidal neurons enabled us to use optical stimulation to preferentially activate relatively sparse unilateral CA3 SC inputs to CA1 neurons in the dorsal hippocampus of anesthetized adult rats. Application of high-intensity, low-frequency conditioning optical stimulation induced robust LTD that was input selective and NMDAR dependent, requiring the GluN2B subunit and the ion channel function of NMDARs. Unlike LTD induced by electrical stimulation, which excites neurons indiscriminately and *en masse*, diffuse selective SC optical LFS-induced LTD was resistant to agents that modulate endogenous mGluR5 or muscarinic AChR activation. Remarkably, although oLTD itself did not appear to be lateralized, AD Aß protein preferentially lowered the threshold to induce LTD at CA3 SC input to CA1 in the left hemisphere in an mGluR5-dependent manner. Taken together, these findings attest that diffuse, strong, low-frequency synaptic activation of CA1 neurons by endogenous glutamate released from CA3 neurons triggers a relatively pure NMDAR-dependent LTD that can be usurped unilaterally by Aß. The apparent lateralization of the facilitation of LTD by Aß opens additional ways of understanding the processes underlying AD at the circuit level.

Consistent with previous *in vitro* research on cortical and hippocampal neurons (El-Gaby et al., 2017; Tchumatchenko et al., 2013; Zhang et al., 2006; Zhang and Oertner, 2007), restricted transduction of ChR2 in less than one third of the CA3 neurons at the site of optical pulse delivery enabled us to diffusely activate synaptic field potentials in the ipsilateral *stratum radiatum* of the CA1 area *in vivo*. Importantly, repetitive diffuse activation of these SCs triggered robust LTD. Unlike the electrical stimulation field, which is expected to radiate relatively uniformly around the tip of the wire electrodes, the optical stimulation should generate a more spatially restricted directional field spreading from the tip of the optical probe (Yizhar et al., 2011). Consistent with the presumed relative independence of the sparsely activated optical pathway and the electrical pathway under the present electrode configuration, the expression of oLFS-induced LTD was input selective, not interacting with comparable LTD of electrically evoked responses recorded in a nearby mixed SC/commissural pathway induced by eLFS. Even though single or repeated eLFS did not induce LTD of the optically evoked synaptic responses, repeated, but not single, eLFS inhibited LTD induction by oLFS. One possible explanation for the latter finding is that repeated eLFS caused sufficient glutamate spillover to activate group II mGluRs, which has been reported to inhibit subsequent LTD induction (Mellentin and Abraham, 2001) (but see Santschi et al., 2006). Although optical, like electrical, stimulation of CA3 neurons activates recurrent collaterals, these connections are extremely sparse, and collateral-induced firing of nearby CA3 neurons is very strongly suppressed by feed-forward inhibition (Guzman et al., 2016; Sun et al., 2017). Similar to electrical conditioning stimulation (Hu et al., 2014), we found that a strong optical conditioning protocol (900 pulses at an intensity evoking a 95% maximum fEPSP) was required to induce robust LTD. Even though application of 900 pulses at 75%, but not at 50%, was sufficient to induce LTD, we chose to vary the number of high-intensity pulses during the oLFS to investigate the mechanisms of LTD induction. Increasing light intensity recruits more ChR2 expressing CA3 neurons (Lin, 2011; Nagel et al., 2003) and should mimic physiological conditions where synaptic activation is strongly synchronized. Such synchronized firing will more effectively depolarize CA1 neurons, which is known to increase the likelihood and magnitude of NMDAR-dependent LTD (Oliet et al., 1997).

Indeed, the oLTD was potently inhibited by NMDAR antagonists acting at the orthosteric glutamate binding site (D-AP5 and CPP), the GluN2B subunit (Ro 25-6981), or the open ion channel (MK-801). Our data provide evidence that GluN2B subunits are critical for oLTD induction *in vivo*, similar to eLTD (Fox et al., 2006; Wong et al., 2007). The ability of the open-channel, use-dependent, NMDAR blocker MK-801 (Harris and Pettit, 2007) to inhibit oLTD indicates that its induction is dependent on ion flux through NMDARs. Contrary to some recent reports

that MK-801 and related agents failed to prevent eLTD *in vitro* (Nabavi et al., 2013), our data support the widely accepted view that relatively slow Ca^{2+} influx through NMDARs results in LTD at hippocampal synapses (Babiec et al., 2014). Because MK-801 blocks the NMDAR channel in a use-dependent manner, it is conceivable that the lack of inhibition of LTD in some studies is because of residual channel activity. Future studies should evaluate the need for metabotropic functions of GluN2B subunits of NMDARs (Nabavi et al., 2013) in LTD induction *in vivo*, and whether there are *in vivo* conditions under which such functions may be sufficient to induce LTD.

Cholinergic activation can enable LTD induction at CA3-to-CA1 synapses (Volk et al., 2007), but its importance in mediating LTD *in vivo* is relatively unexplored. Whereas oLTD was resistant to block by the muscarinic AChR antagonist scopolamine, we confirmed our previous report that the same dose strongly blocks eLTD at 3 hr (Hu et al., 2014). Moreover, whereas boosting cholinergic transmission with the anticholinesterase donepezil greatly facilitated eLTD, it did not significantly affect oLTD induction. These findings are consistent with the idea that the electrical conditioning stimulation was activating significant numbers of medial septal cholinergic fibers as they pass into the hippocampus (Cole and Nicoll, 1983). On the other hand, our oLFS data indicate that cholinergic drive has little influence on LTD induction when apical synapses are diffusely and selectively activated *in vivo*. Interestingly, group I mGluR-dependent LTD at these synapses has been reported to be controlled by muscarinic AChRs activation, possibly by increasing background protein kinase C (PKC) activation (Kamsler et al., 2010). Thus, the differential involvement of muscarinic AChRs may be because we found that LTD induced by oLFS, unlike that induced by eLFS, was apparently independent of mGluR5 activation.

Because mGluR5s on CA1 dendrites are located outside the synapse, especially in the immediate perisynaptic area (Luján et al., 1997), the likelihood of activation of mGluR5s will depend on the spatial pattern of presynaptic activity, being more likely to be activated by dense rather than diffuse stimulation patterns. Electrical field stimulation, as used in the present study and the vast majority of previous studies, provides favorable conditions for accumulation of glutamate at peri- and extra-synaptic sites, due to the close proximity of activated synapses. Consistent with a role of mGluR5 in hippocampal eLTD, negative or positive modulators of mGluR5s, including the doses of MTEP and VU 0360172 used here, can regulate the induction of LTD by electrical LFS at mixed SC/commissural apical synapses *in vivo* (K.J. O'Riordan et al., 2017, BNA, abstract PW115; Popkirov and Manahan-Vaughan, 2011). On the contrary, optical stimulation of more diffuse synaptic inputs will greatly diminish the likelihood of glutamate spillover-mediated activation of mGluRs. The present finding that mGluR5 modulators did not affect oLTD implies that mGluR5s are not essential for LTD at SC input to CA1 under conditions that model more physiological diffuse synaptic activation by endogenously released glutamate *in vivo*. Somewhat similarly, in the cerebellum, the likelihood and mechanisms of LTD induction, including the involvement of group I mGluRs, depend on the spatial pattern of synaptic activation of granule cell inputs to Purkinje cells (Marcaggi and Attwell, 2007).

At the circuit level, we failed to find significant left/right asymmetry of LTD induced at SC apical synapses with CA1 neurons *in vivo*. There is strong evidence of circuit asymmetry at the morphological and molecular levels in mouse hippocampus. In adult mice, left CA3 axons predominantly form small *en passant* synapses onto thin CA1 spines that have a high density of GluN2B subunit-containing NMDARs and, possibly, mGluR5s (Kawakami et al., 2003; Shinohara and Hirase, 2009). In contrast, right CA3 axons mainly form large synapses onto mushroom-type CA1 spines that have a high density of GluA1 subunit-containing α-amino-3-hydroxy-5-methylisoxazolepropionate receptor (AMPARs) (Kawakami et al., 2003; Shinohara and Hirase, 2009). Using optogenetic methods, LTP was found to be primarily inducible at apical synapses with left CA3 axon inputs in adult mouse hippocampal slices (Kohl et al., 2011; Shipton et al., 2014). Although lateralization of LTD has not been reported, LTD is preferentially induced in slices from adult mice that congenitally symmetrically express the large, GluA1-enriched type of apical synapse normally formed by right CA3 SC inputs (Kawahara et al., 2013). Based on these findings, it might be predicted that LTD will be similarly biased to CA1 apical synapses formed by right CA3 pyramidal neurons in wild-type animals. On the other hand, we found that LTD induction by oLFS was GluN2B dependent in the present studies, which might be expected to favor LTD induction at left CA3 inputs to CA1. Regardless, we failed to find evidence for lateralization of LTD induced by either peri-threshold, sub-maximal, or near-maximal oLFS protocols. Perhaps the extent of lateralization in the rat hippocampus of (1) left-side CA3 input to GluN2B-enriched small spines and (2) right-side CA3 input to GluA1-enriched mushroom-type spines is not as strong as that previously reported for mouse CA1 pyramidal neurons.

Although we failed to find evidence for lateralization of oLTD, the threshold for inducing this LTD was lowered asymmetrically by Aß oligomers. The preferential Aß-mediated facilitation of LTD induced by activation of CA1 apical inputs originating in left CA3 pyramidal neurons is likely attributable to a lateralization of mGluR5 as well as GluN2B at these synapses, similar to the mouse hippocampus (Shinohara and Hirase, 2009). Like Aß-facilitated eLTD (Hu et al., 2014), the mGluR5 negative allosteric modulator MTEP inhibited Aß-mediated facilitation of LTD induction by oLFS of left SCs. mGluR5s are believed to be critical for LTD facilitation by Aß oligomers, primarily because they potently and selectively bind to cellular prion protein and mGluR5s to promote the formation of a co-receptor complex with aberrant downstream signaling, including inappropriate activation of GluN2B-containing NMDARs (Hu et al., 2014; Um et al., 2013). Furthermore, in the presence of Aß oligomers, mGluR5s are removed from extrasynaptic sites into the synapse (Renner et al., 2010), making them more likely activated when glutamate is diffusely released from CA3 neurons, as achieved in the present experiments using optical pulses. Future studies should determine whether, like Aß-mediated inhibition of LTP (Minogue et al., 2007), the facilitation of LTD by Aß is increased with aging, and whether similar mGluR5-dependent mechanisms are engaged in the aged rodent brain asymmetrically.

Hippocampal ensembles are likely to be encoded sparsely normally (Ramirez et al., 2013). Using optogenetic methods

such as those developed here offers the opportunity to investigate plasticity induction by synaptic activation of spatial distributions that more closely mimic natural conditions. The finding that robust LTD is induced *in vivo* by relatively diffuse optical synaptic activation makes the study of oLTD especially relevant to the study of core processes underlying hippocampus-dependent behavior. Because hippocampal dysfunction asymmetry is implicated in neurological and psychiatric diseases, the present approach should be particularly helpful in elucidating the pathophysiological mechanisms of these disorders, including AD (Douaud et al., 2013; Hanson et al., 2010; Mondelli et al., 2010; Teicher et al., 2012; Yu et al., 2017). The discovery that Aß-mediated LTD is lateralized in the hippocampus provides a means to reveal additional strategies to interrupt circuit-level disruptions in the amyloidosis of AD.

EXPERIMENTAL PROCEDURES

For a detailed description of the experimental procedures, see the Supplemental Experimental Procedures.

Animals and Surgery

Adult male Wistar and Lister hooded rats were housed in a 12-hr/12-hr light/dark cycle at room temperature (19–22°C). Animal care and experimental protocols were carried out in accordance with the approval and oversight of the Health Products Regulatory Authority, Dublin, Ireland.

For transduction, the animals (10–12 weeks old, 300–330 g) were anesthetized with ketamine (80 mg/kg, i.p.) and xylazine (8 mg/kg, i.p.). A total of 1.0 ± 0.1 μL virus was injected. The animals were monitored until full consciousness was regained and housed singly for 1 week or until wound healing had completed, after which they were housed in pairs with continuous access to food and water *ad libitum*.

Electrode Implantation and Recording *In Vivo*

At the time of electrode implantation/recording under non-recovery anesthesia (urethane, 1.5–1.6 g/kg, i.p.), animals were ~4.5–6 months old (400–500 g). An optrode was lowered into the CA3 area, and a monopolar recording electrode was lowered into the *stratum radiatum* of area CA1.

Alternating optical and electrical test stimulation was delivered every 30 s, each pathway receiving a pulse every 60 s. Unless otherwise stated, LTD was induced using a low-frequency conditioning stimulation protocol of either optical (oLFS) or electrical (eLFS) pulses consisting of 900 stimuli run at 1 Hz, with the intensity increased to evoke potentials that were 95% maximum amplitude. Injections were made, i.c.v., in a 5- to 10-μL volume with a 1.0 μL/min speed.

Fluorescence Imaging

For fluorescence imaging, coronal slices (200 μm thick) were suspended in a solution of DAPI. Images were acquired on an Olympus BX51 upright microscope and a Leica SP8 gated STED microscope.

In order to estimate the density of expression, we carried out pyramidal cell count analysis in the cell-body layer near the injection site. First, we confirmed that nuclear DAPI staining corresponded to pyramidal neurons as detected in adjacent Nissl-stained brain sections. We estimated the number of cell bodies with clear presence of EYFP in a standardized cell-body zone of interest (400 μm long). Cell counts were performed three times, and an average for each panel was taken.

Viral Agents

An AAV vector (serotypes 2 and 5) containing the ChR2 sequence under control of the calcium/calmodulin-dependent protein kinase II (CaMkII) promoter, fused to the gene for EYFP (rAAV/CaMKIIa-hChR2(H134R)-EYFP-WPRE) was used. The plasmid was provided by Dr. Karl Deisseroth (Stanford University). The viral solution (5.1–8.5 – 10^{12} vector genomes [vg]/mL) was prepared by the University of North Carolina Vector Core (Chapel Hill, NC, USA). Upon arrival, the sample was separated on ice into 3-μL aliquots and stored at −80°C.

Pharmacological Agents

D-AP5, CPP, MTEP, scopolamine, MK-801, and donepezil were prepared in ultra-clean water and diluted in saline. Ro 25-6981 was dissolved in DMSO and diluted in saline. VU 0360172 was dissolved in 10% Tween-80 in saline. LY341495 was dissolved in 1.2 M equivalent NaOH and diluted in saline. Chemical names, suppliers, and dose choice rationale are provided in the Supplemental Experimental Procedures.

Aβ-derived diffusible ligands (ADDLs) were used to study the effects of synaptotoxic Aβ aggregates. They were prepared as described previously (Hu et al., 2014).

Data Analysis

Values are expressed as the mean percent (± SEM) baseline fEPSP amplitude. Similar results were obtained when fEPSP slope was analyzed. The average of either a 30- or 60-min recording period (i.e., 30 or 60 fEPSP sweeps), starting before the normal time of injection, was used to calculate the baseline value. The last 10 min prior to LFS was used to calculate the pre-induction fEPSP amplitude. Unless otherwise stated, the magnitude of LTD was measured over the last 10 min at 1 or 3 hr post-LFS. Control experiments were interleaved randomly throughout. For two groups with two time points, a 2WA-RM-B was used. To compare between groups of three, a one-way ANOVA with Bonferroni multiple comparisons was used. To compare between time points of three or more, one-way repeated-measures ANOVA with Bonferroni multiple comparisons (1WA-RM-B) was used. A two-tailed paired Student's t test (paired t), with Bonferroni correction in the case of multiple post hoc tests, was used to compare between "Pre" and "Post" within groups. A value of $p < 0.05$ was considered statistically significant.

SUPPLEMENTAL INFORMATION

Supplemental Information includes Supplemental Experimental Procedures and seven figures and can be found with this article online at https://doi.org/10.1016/j.celrep.2018.01.085.

ACKNOWLEDGMENTS

We thank Patrick Monahan for help with developing the optogenetic methodology. The rAAV plasmid was kindly provided by Dr. Karl Deisseroth (Stanford University). Dr. Gavin McManus assisted us with the fluorescence imaging. This work was supported by Science Foundation Ireland (14/IA/2571) and the Irish Health Research Board (HRA-POR-2015-1102) to M.J.R. and by the National Natural Science Foundation of China (no. 81471114) to N.-W.H.

AUTHOR CONTRIBUTIONS

K.J.O., N.-W.H., and M.J.R. conceived the study and designed the research. K.J.O. and N.-W.H. performed and analyzed *in vivo* experiments. K.J.O., N.-W.H., and M.J.R. wrote the paper.

DECLARATION OF INTERESTS

The authors declare no competing interests.

Received: August 24, 2017
Revised: December 16, 2017
Accepted: January 26, 2018
Published: February 20, 2018

REFERENCES

Andersen, N., Krauth, N., and Nabavi, S. (2017). Hebbian plasticity in vivo: relevance and induction. Curr. Opin. Neurobiol. *45*, 188–192.

Arnth-Jensen, N., Jabaudon, D., and Scanziani, M. (2002). Cooperation between independent hippocampal synapses is controlled by glutamate uptake. Nat. Neurosci. *5*, 325–331.

Babiec, W.E., Guglietta, R., Jami, S.A., Morishita, W., Malenka, R.C., and O'Dell, T.J. (2014). Ionotropic NMDA receptor signaling is required for the induction of long-term depression in the mouse hippocampal CA1 region. J. Neurosci. *34*, 5285–5290.

Bond, A., Jones, N.M., Hicks, C.A., Whiffin, G.M., Ward, M.A., O'Neill, M.F., Kingston, A.E., Monn, J.A., Ornstein, P.L., Schoepp, D.D., et al. (2000). Neuroprotective effects of LY379268, a selective mGlu2/3 receptor agonist: investigations into possible mechanism of action in vivo. J. Pharmacol. Exp. Ther. *294*, 800–809.

Caruana, D.A., Warburton, E.C., and Bashir, Z.I. (2011). Induction of activity-dependent LTD requires muscarinic receptor activation in medial prefrontal cortex. J. Neurosci. *31*, 18464–18478.

Cole, A.E., and Nicoll, R.A. (1983). Acetylcholine mediates a slow synaptic potential in hippocampal pyramidal cells. Science *221*, 1299–1301.

Collingridge, G.L., Peineau, S., Howland, J.G., and Wang, Y.T. (2010). Long-term depression in the CNS. Nat. Rev. Neurosci. *11*, 459–473.

Concha, M.L., Bianco, I.H., and Wilson, S.W. (2012). Encoding asymmetry within neural circuits. Nat. Rev. Neurosci. *13*, 832–843.

De Strooper, B., and Karran, E. (2016). The cellular phase of Alzheimer's disease. Cell *164*, 603–615.

Douaud, G., Menke, R.A., Gass, A., Monsch, A.U., Rao, A., Whitcher, B., Zamboni, G., Matthews, P.M., Sollberger, M., and Smith, S. (2013). Brain microstructure reveals early abnormalities more than two years prior to clinical progression from mild cognitive impairment to Alzheimer's disease. J. Neurosci. *33*, 2147–2155.

El-Gaby, M., Kohl, M.M., and Paulsen, O. (2017). Optogenetic methods to study lateralized synaptic function. In Lateralized Brain Functions Neuromethods, Volume 122, L. Rogers and G. Vallortigara, eds. (Humana Press), pp. 331–365.

Errington, M.L., Bliss, T.V., Richter-Levin, G., Yenk, K., Doyère, V., and Laroche, S. (1995). Stimulation at 1-5 Hz does not produce long-term depression or depotentiation in the hippocampus of the adult rat in vivo. J. Neurophysiol. *74*, 1793–1799.

Fox, C.J., Russell, K.I., Wang, Y.T., and Christie, B.R. (2006). Contribution of NR2A and NR2B NMDA subunits to bidirectional synaptic plasticity in the hippocampus in vivo. Hippocampus *16*, 907–915.

Guzman, S.J., Schlögl, A., Frotscher, M., and Jonas, P. (2016). Synaptic mechanisms of pattern completion in the hippocampal CA3 network. Science *353*, 1117–1123.

Hanson, K.L., Medina, K.L., Nagel, B.J., Spadoni, A.D., Gorlick, A., and Tapert, S.F. (2010). Hippocampal volumes in adolescents with and without a family history of alcoholism. Am. J. Drug Alcohol Abuse *36*, 161–167.

Harris, A.Z., and Pettit, D.L. (2007). Extrasynaptic and synaptic NMDA receptors form stable and uniform pools in rat hippocampal slices. J. Physiol. *584*, 509–519.

Hu, N.W., Nicoll, A.J., Zhang, D., Mably, A.J., O'Malley, T., Purro, S.A., Terry, C., Collinge, J., Walsh, D.M., and Rowan, M.J. (2014). mGlu5 receptors and cellular prion protein mediate amyloid-β-facilitated synaptic long-term depression in vivo. Nat. Commun. *5*, 3374.

Kamsler, A., McHugh, T.J., Gerber, D., Huang, S.Y., and Tonegawa, S. (2010). Presynaptic m1 muscarinic receptors are necessary for mGluR long-term depression in the hippocampus. Proc. Natl. Acad. Sci. USA *107*, 1618–1623.

Kasza, Á., Penke, B., Frank, Z., Bozsó, Z., Szegedi, V., Hunya, Á., Németh, K., Kozma, G., and Fülöp, L. (2017). Studies for improving a rat model of Alzheimer's disease: icv administration of well-characterized β-amyloid 1-42 oligomers induce dysfunction in spatial memory. Molecules *22*, E2007.

Kawahara, A., Kurauchi, S., Fukata, Y., Martínez-Hernández, J., Yagihashi, T., Itadani, Y., Sho, R., Kajiyama, T., Shinzato, N., Narusuye, K., et al. (2013). Neuronal major histocompatibility complex class I molecules are implicated in the generation of asymmetries in hippocampal circuitry. J. Physiol. *591*, 4777–4791.

Kawakami, R., Shinohara, Y., Kato, Y., Sugiyama, H., Shigemoto, R., and Ito, I. (2003). Asymmetrical allocation of NMDA receptor epsilon2 subunits in hippocampal circuitry. Science *300*, 990–994.

Kemp, A., and Manahan-Vaughan, D. (2004). Hippocampal long-term depression and long-term potentiation encode different aspects of novelty acquisition. Proc. Natl. Acad. Sci. USA *101*, 8192–8197.

Kingston, A.E., Ornstein, P.L., Wright, R.A., Johnson, B.G., Mayne, N.G., Burnett, J.P., Belagaje, R., Wu, S., and Schoepp, D.D. (1998). LY341495 is a nanomolar potent and selective antagonist of group II metabotropic glutamate receptors. Neuropharmacology *37*, 1–12.

Kohl, M.M., Shipton, O.A., Deacon, R.M., Rawlins, J.N., Deisseroth, K., and Paulsen, O. (2011). Hemisphere-specific optogenetic stimulation reveals left-right asymmetry of hippocampal plasticity. Nat. Neurosci. *14*, 1413–1415.

Koss, D.J., Jones, G., Cranston, A., Gardner, H., Kanaan, N.M., and Platt, B. (2016). Soluble pre-fibrillar tau and β-amyloid species emerge in early human Alzheimer's disease and track disease progression and cognitive decline. Acta Neuropathol. *132*, 875–895.

Kristofiková, Z., Stástný, F., Bubeniková, V., Druga, R., Klaschka, J., and Spaniel, F. (2004). Age- and sex-dependent laterality of rat hippocampal cholinergic system in relation to animal models of neurodevelopmental and neurodegenerative disorders. Neurochem. Res. *29*, 671–680.

Li, S., Hong, S., Shepardson, N.E., Walsh, D.M., Shankar, G.M., and Selkoe, D. (2009). Soluble oligomers of amyloid Beta protein facilitate hippocampal long-term depression by disrupting neuronal glutamate uptake. Neuron *62*, 788–801.

Lin, J.Y. (2011). A user's guide to channelrhodopsin variants: features, limitations and future developments. Exp. Physiol. *96*, 19–25.

Luján, R., Roberts, J.D., Shigemoto, R., Ohishi, H., and Somogyi, P. (1997). Differential plasma membrane distribution of metabotropic glutamate receptors mGluR1 alpha, mGluR2 and mGluR5, relative to neurotransmitter release sites. J. Chem. Neuroanat. *13*, 219–241.

Marcaggi, P., and Attwell, D. (2007). Short- and long-term depression of rat cerebellar parallel fibre synaptic transmission mediated by synaptic crosstalk. J. Physiol. *578*, 545–550.

Mellentin, C., and Abraham, W.C. (2001). Priming stimulation of group II metabotropic glutamate receptors inhibits the subsequent induction of rat hippocampal long-term depression in vitro. Neurosci. Lett. *307*, 13–16.

Minogue, A.M., Lynch, A.M., Loane, D.J., Herron, C.E., and Lynch, M.A. (2007). Modulation of amyloid-beta-induced and age-associated changes in rat hippocampus by eicosapentaenoic acid. J. Neurochem. *103*, 914–926.

Mondelli, V., Pariante, C.M., Navari, S., Aas, M., D'Albenzio, A., Di Forti, M., Handley, R., Hepgul, N., Marques, T.R., Taylor, H., et al. (2010). Higher cortisol levels are associated with smaller left hippocampal volume in first-episode psychosis. Schizophr. Res. *119*, 75–78.

Nabavi, S., Kessels, H.W., Alfonso, S., Aow, J., Fox, R., and Malinow, R. (2013). Metabotropic NMDA receptor function is required for NMDA receptor-dependent long-term depression. Proc. Natl. Acad. Sci. USA *110*, 4027–4032.

Nagel, G., Szellas, T., Huhn, W., Kateriya, S., Adeishvili, N., Berthold, P., Ollig, D., Hegemann, P., and Bamberg, E. (2003). Channelrhodopsin-2, a directly light-gated cation-selective membrane channel. Proc. Natl. Acad. Sci. USA *100*, 13940–13945.

Oliet, S.H., Malenka, R.C., and Nicoll, R.A. (1997). Two distinct forms of long-term depression coexist in CA1 hippocampal pyramidal cells. Neuron *18*, 969–982.

Ornstein, P.L., Bleisch, T.J., Arnold, M.B., Kennedy, J.H., Wright, R.A., Johnson, B.G., Tizzano, J.P., Helton, D.R., Kallman, M.J., Schoepp, D.D., and Hérin, M. (1998). 2-substituted (2SR)-2-amino-2-((1SR,2SR)-2-carboxycycloprop-1-yl) glycines as potent and selective antagonists of group II metabotropic glutamate receptors. 2. Effects of aromatic substitution, pharmacological characterization, and bioavailability. J. Med. Chem. *41*, 358–378.

Popkirov, S.G., and Manahan-Vaughan, D. (2011). Involvement of the metabotropic glutamate receptor mGluR5 in NMDA receptor-dependent, learning-facilitated long-term depression in CA1 synapses. Cereb. Cortex *21*, 501–509.

Ramirez, S., Liu, X., Lin, P.A., Suh, J., Pignatelli, M., Redondo, R.L., Ryan, T.J., and Tonegawa, S. (2013). Creating a false memory in the hippocampus. Science *341*, 387–391.

Renner, M., Lacor, P.N., Velasco, P.T., Xu, J., Contractor, A., Klein, W.L., and Triller, A. (2010). Deleterious effects of amyloid beta oligomers acting as an extracellular scaffold for mGluR5. Neuron *66*, 739–754.

Santschi, L.A., Zhang, X.L., and Stanton, P.K. (2006). Activation of receptors negatively coupled to adenylate cyclase is required for induction of long-term synaptic depression at Schaffer collateral-CA1 synapses. J. Neurobiol. *66*, 205–219.

Scimemi, A., Fine, A., Kullmann, D.M., and Rusakov, D.A. (2004). NR2B-containing receptors mediate cross talk among hippocampal synapses. J. Neurosci. *24*, 4767–4777.

Shinohara, Y., and Hirase, H. (2009). Size and receptor density of glutamatergic synapses: a viewpoint from left-right asymmetry of CA3-CA1 connections. Front. Neuroanat. *3*, 10.

Shinohara, Y., Hosoya, A., Yahagi, K., Ferecskó, A.S., Yaguchi, K., Sík, A., Itakura, M., Takahashi, M., and Hirase, H. (2012). Hippocampal CA3 and CA2 have distinct bilateral innervation patterns to CA1 in rodents. Eur. J. Neurosci. *35*, 702–710.

Shipton, O.A., El-Gaby, M., Apergis-Schoute, J., Deisseroth, K., Bannerman, D.M., Paulsen, O., and Kohl, M.M. (2014). Left-right dissociation of hippocampal memory processes in mice. Proc. Natl. Acad. Sci. USA *111*, 15238–15243.

Sperling, R., Mormino, E., and Johnson, K. (2014). The evolution of preclinical Alzheimer's disease: implications for prevention trials. Neuron *84*, 608–622.

Spires-Jones, T.L., and Hyman, B.T. (2014). The intersection of amyloid beta and tau at synapses in Alzheimer's disease. Neuron *82*, 756–771.

Staubli, U., and Scafidi, J. (1997). Studies on long-term depression in area CA1 of the anesthetized and freely moving rat. J. Neurosci. *17*, 4820–4828.

Sun, Q., Sotayo, A., Cazzulino, A.S., Snyder, A.M., Denny, C.A., and Siegelbaum, S.A. (2017). Proximodistal heterogeneity of hippocampal CA3 pyramidal neuron intrinsic properties, connectivity, and reactivation during memory recall. Neuron *95*, 656–672.e53.

Tchumatchenko, T., Newman, J.P., Fong, M.F., and Potter, S.M. (2013). Delivery of continuously-varying stimuli using channelrhodopsin-2. Front. Neural Circuits *7*, 184.

Teicher, M.H., Anderson, C.M., and Polcari, A. (2012). Childhood maltreatment is associated with reduced volume in the hippocampal subfields CA3, dentate gyrus, and subiculum. Proc. Natl. Acad. Sci. USA *109*, E563–E572.

Titley, H.K., Brunel, N., and Hansel, C. (2017). Toward a neurocentric view of learning. Neuron *95*, 19–32.

Um, J.W., Kaufman, A.C., Kostylev, M., Heiss, J.K., Stagi, M., Takahashi, H., Kerrisk, M.E., Vortmeyer, A., Wisniewski, T., Koleske, A.J., et al. (2013). Metabotropic glutamate receptor 5 is a coreceptor for Alzheimer aβ oligomer bound to cellular prion protein. Neuron *79*, 887–902.

Volk, L.J., Pfeiffer, B.E., Gibson, J.R., and Huber, K.M. (2007). Multiple Gq-coupled receptors converge on a common protein synthesis-dependent long-term depression that is affected in fragile X syndrome mental retardation. J. Neurosci. *27*, 11624–11634.

Wachinger, C., Salat, D.H., Weiner, M., and Reuter, M.; Alzheimer's Disease Neuroimaging Initiative (2016). Whole-brain analysis reveals increased neuroanatomical asymmetries in dementia for hippocampus and amygdala. Brain *139*, 3253–3266.

Wong, T.P., Howland, J.G., Robillard, J.M., Ge, Y., Yu, W., Titterness, A.K., Brebner, K., Liu, L., Weinberg, J., Christie, B.R., et al. (2007). Hippocampal long-term depression mediates acute stress-induced spatial memory retrieval impairment. Proc. Natl. Acad. Sci. USA *104*, 11471–11476.

Xu, L., Anwyl, R., and Rowan, M.J. (1997). Behavioural stress facilitates the induction of long-term depression in the hippocampus. Nature *387*, 497–500.

Yizhar, O., Fenno, L.E., Davidson, T.J., Mogri, M., and Deisseroth, K. (2011). Optogenetics in neural systems. Neuron *71*, 9–34.

Yu, M., Engels, M.M.A., Hillebrand, A., van Straaten, E.C.W., Gouw, A.A., Teunissen, C., van der Flier, W.M., Scheltens, P., and Stam, C.J. (2017). Selective impairment of hippocampus and posterior hub areas in Alzheimer's disease: an MEG-based multiplex network study. Brain *140*, 1466–1485.

Zhang, Y.P., and Oertner, T.G. (2007). Optical induction of synaptic plasticity using a light-sensitive channel. Nat. Methods *4*, 139–141.

Zhang, F., Wang, L.P., Boyden, E.S., and Deisseroth, K. (2006). Channelrhodopsin-2 and optical control of excitable cells. Nat. Methods *3*, 785–792.